

Supplementary Information

Modulating the visible emission and whispering gallery mode lasing through the self-induced defects in a Ga-doped ZnO tapered microcavity

Rubia Anwar¹, Cuong Ton-That², and M. Azizar Rahman^{1,*}

¹*Department of Physics, Bangladesh University of Engineering and Technology, Old Academic Building, Dhaka-1000, Bangladesh*

²*School of Mathematical and Physical Sciences, University of Technology Sydney, Ultimo, NSW 2007, Australia*

*Corresponding author. Email: azizar@phy.buet.ac.bd

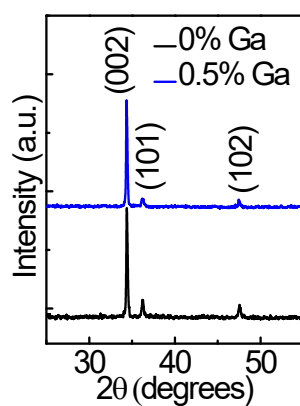


Fig.S1. XRD of undoped and Ga-doped ZnO nanorods. XRD patterns for pristine and GZO nanorods show reflections consistent with wurtzite ZnO and a preferred (002) orientation.

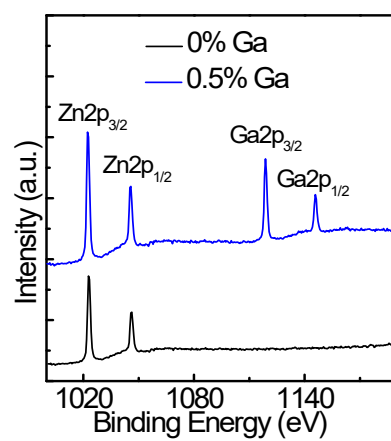


Fig. S2. X-ray photoelectron spectroscopy of pristine and GZO microrods. XPS core level spectra confirming Ga incorporation in the microrods.

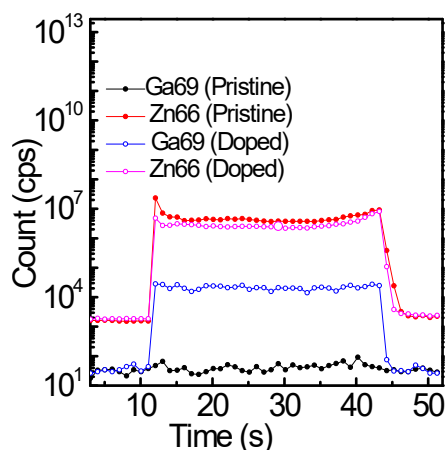


Fig. S3. LA-ICP-MS depth profiles confirming Ga incorporation. Time-dependent LA-ICP-MS signals (laser crater $100\ \mu\text{m}$, scan $100\ \mu\text{m s}^{-1}$, fluence $4.35\ \text{J cm}^{-2}$, 10 s runoff) for Zn-66 and Ga-69 in pristine versus Ga-doped nanorods. Ga is detected only in doped samples, with stable signals over the ablation interval, consistent with incorporation through the probed depth. This is for 0.13% Ga-doped ZnO nanorods.

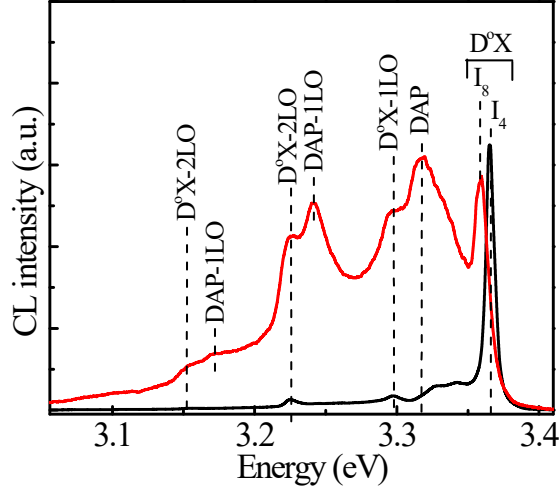


Fig. S4. Near-band-edge (NBE) CL spectra of undoped and GZO microrods at 80 K. CL spectra highlighting donor-bound exciton ($D^{\circ}X$) and donor–acceptor pair (DAP) features with assigned I_4 and I_8 lines and their LO-phonon replicas (e.g., $D^{\circ}X$ -1LO/2LO, DAP-1LO). The presence of well-resolved NBE lines indicates preserved excitonic quality upon Ga doping.

Table S1: The steady state spectra are simulated using equation (A1) of Ref^[1]. The table show the value of fitting parameters value; where, photon energy ($\hbar\omega$), longitudinal optical phonon ($\hbar\omega_{LO}$), the number of phonon (n), the electron-phonon coupling strength (S), zero phonon energy (E_{ZPL}) and represents the FWHM of the phonon side band (σ).

Emission	$\hbar\omega_{LO}$ (eV)	E_{ZPL} (eV)	σ (eV)	S
Green	70 ± 0.1	2.81 ± 0.01	0.16 ± 0.01	5.8 ± 0.05
Yellow	70 ± 0.1	2.7 ± 0.02	$0.24 \pm 0.003 \text{ eV}$	7.1 ± 0.1

Table S2. Multi-exponential TRPL fit parameters for green and yellow emission. Lifetimes τ_i and amplitudes A_i from multi-exponential fits to the time-resolved PL decays of the green and yellow bands. The microsecond-scale components are consistent with defect-mediated recombination; amplitudes A_i provide the fractional contribution of each channel.

Emissions	τ_1 (μs)	τ_2 (μs)	τ_3 (μs)	A_1	A_2	A_3
Green	0.68	2.7	7.44	0.11	0.10	0.04
Yellow	0.72	3.90	36.56	0.24	0.022	0.0019

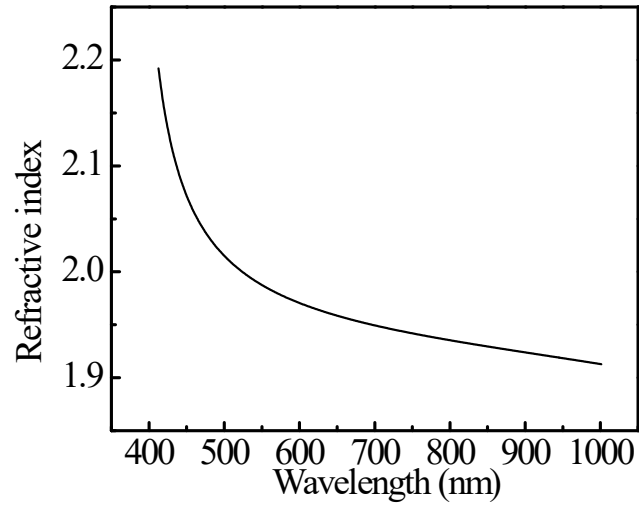


Fig. S5. Wavelength-dependent refractive index $n(\lambda)$ of ZnO (TE polarization). Index values were extracted by fitting measured data with a Sellmeier model and the resulting $n(\lambda)$ was used in the mode simulations.

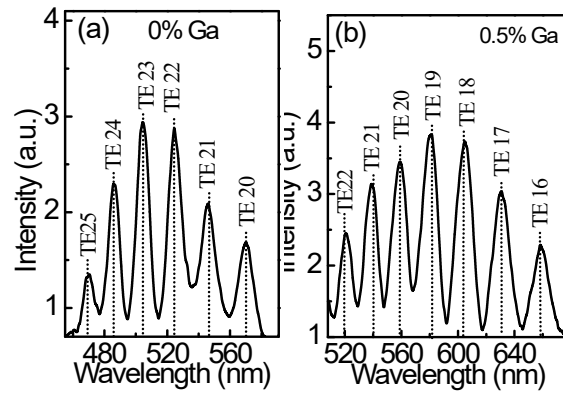


Fig. S6. Enlarged views highlighting discrete resonances: (a) Undoped microrod (460 – 590 nm) and (b) GZO microrod (515 – 680 nm). Dashed lines denote TE-polarized modes.

References

- [1] C. Spindler, F. Babbe, M. H. Wolter, F. Ehré, K. Santhosh, P. Hilgert, F. Werner, S. Siebentritt, *Phys. Rev. Mater.* **2019**, 3, 090302.